Journal of Zhejiang University SCIENCE A
ISSN 1673-565X (Print); ISSN 1862-1775 (Online)
www.zju.edu.cn/jzus; www.springerlink.com
E-mail: jzus@zju.edu.cn

Mesoscopic analysis of the utilization of hardening model for a description of softening behavior based on disturbed state concept theory

Jian-ye ZHENG[†1], An-li WU[2]

([1]*Guangzhou Metropolis Construction Commission, Guangzhou 510030, China*)

([2]*College of Civil Engineering and Architecture, Inner Mongolia University of Technology, Hohhot 010051, China*)

[†]E-mail: zhengjianye@sjtu.org

Received Nov. 5, 2007; revision accepted May 16, 2008

Abstract: Mesoscopic characteristics of a clayey soil specimen subjected to macroscopic loading are examined using a medical-use computerized tomography (CT) instrument. Disturbed state concept (DSC) theory is based on the utilization of the hardening model. DSC indirectly describes material behavior by claiming that the actual response of the material is expressed in terms of the relative intact (RI) response and the fully adjusted (FA) response. The occurrence of mesoscopic structural changes of material has similarities with the occurrence of a macroscopic response of the material under loadings. In general, the relative changing value of a softening material is three to five times more than that of a hardening material. Whether special zones exist or not in a specimen cross section does not affect the following conclusion: hardening material and softening material show mechanical differences with CT statistical indices values prominently changing, and the change is related to the superposing of a disturbance factor. A new disturbance factor evolution function is proposed. Thus, mesoscopic statistical indices are introduced to describe macroscopic behavior through the new evolution function. An application of the new evolution function proves the effectiveness of the amalgamation of a macroscopic and a mesoscopic experimental phenomenon measurement methods.

Key words: Constitutive model, Disturbed state concept (DSC), Computerized tomography (CT), Softening
doi:10.1631/jzus.A0720062 **Document code:** A **CLC number:** TU452

INTRODUCTION

Geologic media are modeled using empirical techniques or models that have limited capabilities. Sometimes it is inconvenient to choose only one constitutive model to depict material response. Disturbed state concept (DSC) theory can characterize material response indirectly by utilizing one or two constitutive models. DSC claims that the actual response of the material subjected to loadings is the weighted average value of two reference responses, namely the relative intact (RI) response and the fully adjusted (FA) response (Desai, 2001). A disturbance factor D plays the role of the weight factor and is defined to express actual response (AR) in terms of RI response and FA response. RI response acts as the original perfection and is assumed to harden continuously. FA response is the defined limitation and can be assumed to act as voids, such as in continuum damage mechanics (Katti and Desai, 1995). The loadings make the mesoscopic structure of the material change. Mechanically perfect parts (RI) of material transform to limitation parts (FA), and the coalescence of these two types of response provides the expected result.

In China regarding DSC studies on rock mechanics, e.g., Wu and Zhang (2004) have presented the unloading failure characteristics of a rock mass by DSC; Wang and Ge (2004) discussed parameter determination and optimization of the hierarchical single surface (HISS) model which is widely used within the framework of DSC. Regarding DSC studies on

soil mechanics, Zhou *et al*.(2004) proposed a DSC model to describe the hypo-plasticity behavior of structured soil; Wang *et al*.(2004) promoted a DSC method to perform a structural clay transformation ability analysis; Zhang *et al*.(2005) implemented DSC on a study of a cohesive soil stress-strain relationship and compressive deformation. Overseas, the explanations of the DSC mechanism by Desai *et al*.(1995) and Desai and Toth (1996) led to the introduction of a nondestructive acoustic method or ultrasonic velocity measurement method to associate macroscopic response with physical characteristics as supportive discussions on DSC origin; Michael (2001) put forward a sound wave method to predict the stress-strain response of cement-based materials in the infrastructure.

UTILIZATION OF THE HARDENING MODEL FOR SOFTENING RESPONSE DESCRIPTION

In DSC, RI can be defined or described by linear elastic, nonlinear elastic, plasto-elastic, or any other suitable model (Erkens, 2002). FA can be defined as a more fragile RI or, in other words, can be supposed to bear loadings like RI does, with the same kind of stress-strain relationship but with a much lower ability (Desai, 2001; Frantziskonis, 1987a). The stress tensor of AR is given by

$$\sigma_{ij}^{\mathrm{AR}} = (1-D)\sigma_{ij}^{\mathrm{RI}} + D\sigma_{ij}^{\mathrm{FA}}. \tag{1}$$

It is assumed that the strains are the same in the RI, FA and AR parts. The evolution function of D is

$$D = D_{\mathrm{u}}(1-\mathrm{e}^{-A\xi_D^Z}), \tag{2}$$

where A, Z and D_{u} are material parameters. The independent variable in Eq.(2) is an effective plastic deviatoric strain of the material:

$$\xi_D = \int (\mathrm{d}\varepsilon_{ij}^{\mathrm{p}}\mathrm{d}\varepsilon_{ij}^{\mathrm{p}})^{1/2}, \tag{3}$$

where $\mathrm{d}\varepsilon_{ij}^{\mathrm{p}}$ is an increment of plastic deviatoric strain. The models chosen for the RI or FA response description pertain to hardening constitutive models, but the weighted average value of the descriptions can comport with the softening response (Frantziskonis, 1987b). This paper claims that both hardening material and softening material do experience disturbance, but compared to softening material, hardening material undergoes a less "disturbing" one that is trivial enough to neglect. "Disturbance" is defined as having the same meaning as "mesoscopic structural changes", and such an approximation is followed thus: hardening material has no modification in their state such as decay or degradation occurring, while softening material has modifications occurring. A hardening response superposed with a disturbance factor D displays softening behavior. D determines the proportion of the material part of RI to the material part of FA, and the evolution process of D is parallel to the process of the RI part degrading to the FA part. If the mesoscopic structure does not change, in other words, if no disturbance happens, D is identically equal to 0, and Eq.(1) degenerates to be

$$\sigma_{ij}^{\mathrm{AR}} = \sigma_{ij}^{\mathrm{RI}}, \tag{4}$$

which shows that only RI is used for the hardening response description. D makes it possible to characterize a softening response over a hardening model.

COMBINATION OF MESOSCOPIC EXPERIMENT AND MACROSCOPIC EXPERIMENT

Computerized tomography (CT) scanning has been widely used for medical purposes and developed as a nondestructive method for engineering materials. The CT scanner was developed for industrial purposes in such a way that the X-ray capacity is much higher than that used in a medical environment. We can say that CT is a quantitative measurement technology based on digital techniques, which is used to detect and describe the sectional characteristics of tested materials (Sun, 2002). The density change in the clayey soil specimen can be investigated. 2D cross-sectional images of the deformed specimen are obtained, the behavior in the soil is not only visualized but also evaluated quantitatively, and the digital index (CT statistical datum) is defined and established from scanning results, which show the changes of material mesoscopic structure.

The deformation characteristics of silty clay subjected to tri-axial loading are studied using real-time CT scanning. The following equations show the relationship between the transmissibility of X-rays and material density. μ_m is the attenuation coefficient to the X-ray of per unit tested material mass. ρ is the density of the tested material. CT-value H is defined as a direct ratio to μ:

$$H = k\mu_m\rho. \tag{5}$$

Given a known μ_m, we can see that the change in H stands for a change of ρ. This paper claims that the density change reflects the change in the mesoscopic structure of the material, i.e., the changing of material mesoscopic structure causes H to change. The development of disturbance D corresponds with the development of material mesoscopic characteristic changes, and H's changing can be the reflection of material mesoscopic characteristic changes. Thus, mesoscopic structural changes can be visualized. It is emphasized that the purpose of CT measurement was not imaging but measuring transmission intensities.

Multifunctional tri-axial loading devices are used to conduct undrained consolidation shearing loading tests. At the same time, the SIEMENS SOMATOM+CT instrument system is utilized for the mesoscopic experiment according to the macroscopic compressing loading test. Additionally, the tri-axial compression experiment is carried out by the multifunctional experiment system. CT scanning is carried out simultaneously with the compressive loading test (Sun *et al*., 2004). It is actually an image taking and a CT-value counting process matching with the compressive loading course.

The course of the experiment proceeds as follows: (1) determination of parameters for experiment system and scanning time presetting; (2) specimen allocation; (3) fine adjustment of the specimen location for proper scanning stratum position fixing; (4) conducting scanning; (5) fine adjustment of the specimen position or the scanning instrument for maintenance of the same fixed position of the scanning stratum; (6) conducting scanning and position adjustment until the end of the experiment.

Fig.1 illustrates the fixed position of scanning stratums for the clayey soil specimen which is settled in a nonmetal obdurate compressive cell. The specimen cylinder is 61.8 mm in diameter and 125 mm in height. In Fig.1, the dark area at the center represents the specimen and the bright area is the empty room of the compressive cell. The dark area along the margins represents the compressive cell. Table 1 provides the typical physico-mechanical index parameters of two kinds of clayey soils, i.e., clay and soil clay.

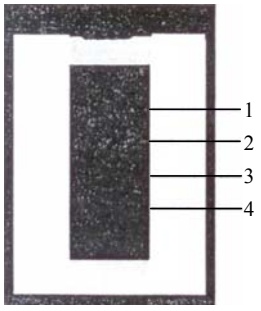

Fig.1 Scanning stratums 1~4 of specimen in the nonmetal obdurate compressive cell

Table 1 Physico-mechanical indices of clayey soil

Clayey soil	Water content w (%)	Unit weight γ (kN/m^3)	Void ratio e
Clay	34.1	18.5	0.972
Silty clay	26.7	19.2	0.776
Clayey soil	**Saturation S_r (%)**	**Specific weight G_s**	**Plasticity index I_p**
Clay	95.5	2.72	18.5
Silty clay	92.9	2.70	13.5

At the beginning the X-ray source and detector moves along a little and rotates a little around the specimens at the specified depths to find the fixed position of scanning stratums. The fixed positions are then marked and traced to make sure that the same position is scanned during the whole experiment (Sun *et al*., 2004). n points on each of the four stratums of the specimen are required for CT statistical data extraction. The mean of the CT-value for these 4n points is assigned as the mean of the CT-value of the entire specimen:

$$\bar{H} = \frac{1}{4n}\sum_{j=1}^{4}\sum_{i=1}^{n}H_{ij}. \tag{6}$$

On the jth (j=1~4) stratum, mean of H for these n points is

$$\bar{H}_j = \frac{1}{n}\sum_{i=1}^{n}H_i, \tag{7}$$

on one of the stratums, variance of H for these n points is

$$\delta_H=\sqrt{\frac{1}{n-1}\sum_{i=1}^{n}(H_i-\bar{H})^2}. \tag{8}$$

In Eqs.(6)~(8) $\bar{H}$, $\bar{H}_j$ and δ_H are defined as the statistical indices for measurement of inner mesoscopic changing of material. $\bar{H}$ gives expression to mesoscopic structural changes of the tested material, and δ_H represents the acuity of the mesoscopic structural changes.

CORRESPONDENCE OF MESOSCOPIC PHENOMENON AND MACROSCOPIC PHENOMENON

Scanning results of specimen continuity

Fig.2 demonstrates the stress-strain relationship of two typical Shanghai grey clayey soils—clay and silty clay. Fig.3 shows these two soils' mesoscopic parameters—statistical indices of real-time CT scanning in phases in accordance with the overall traditional tri-axial undrained consolidation test under compressive loading and the change of one of the mesoscopic indices, namely, CT-value. The relative changing values of $\bar{H}$, $\bar{H}_j$ and δ_H are defined by

$$\Delta\bar{H}'=\frac{\bar{H}_{\max}-\bar{H}_{\min}}{\bar{H}_{\min}}\times 100\%, \tag{9}$$

$$\Delta\bar{H}_j'=\frac{\bar{H}_{j\max}-\bar{H}_{j\min}}{\bar{H}_{j\min}}\times 100\%, \tag{10}$$

$$\Delta\delta_H'=\frac{\delta_{H\max}-\delta_{H\min}}{\delta_{H\min}}\times 100\%. \tag{11}$$

The relative changing value evaluates the maximum extent of the changes of $\bar{H}$, $\bar{H}_j$ and δ_H. Fig.3 reveals that the mean CT-values of both hardening clay and hardening silty clay progress with tiny variation which can almost be neglected, while the

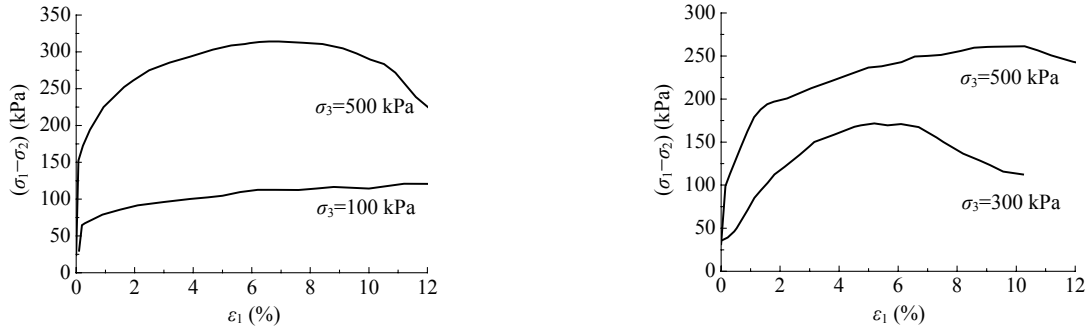

Fig.2 Stress-strain relationship. (a) Clay; (b) Silty clay

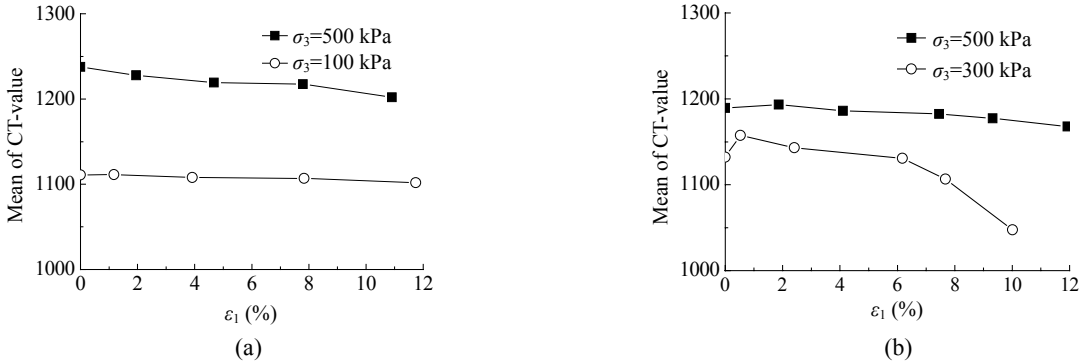

Fig.3 Mean of CT-value ($\bar{H}$) of entire specimen. (a) Clay; (b) Silty clay

mean CT-value of both softening clay and softening silty clay steadily decreases. Table 2 indicates that the relative changing value $\Delta\bar{H}'$ of softening clay is almost three times more than that of hardening clay, while $\Delta\bar{H}'$ of softening silty clay is five times more than that of hardening silty clay.

The relative changing values of scanning stratums 1~4 in hardening and softening silty clays (Figs.4~5 and Table 3) show that the relative changing value of hardening material is far less than that of softening material. $\Delta\bar{H}'_j$ and $\Delta\delta'_H$ of softening material are usually five times more than that of hardening material. In particular, in Fig.4b, the data of Stratum 3 shows abnormality and thus can be taken out of consideration, but the data of all the stratums-distinctly give evidence of the regulation aforementioned.

Eq.(1) holds that disturbance factor D be superposed on the hardening response to obtain a softening behavior description, so the mesoscopic statistical indices are brought into the explanation of the macroscopic phenomenon: when it is unnecessary to consider D, the relative changing value is often too small to take into account; but when it is necessary to superpose D on the hardening response to describe the softening response, the relative changing value is large enough and can not be neglected.

Table 2 Relative changing value of mean of CT-value $\bar{H}$

Entire specimen	$\Delta\bar{H}'$ (%)	
	Hardening	Softening
Clay	1.1	3.0
Silty clay	1.8	10.5

Table 3 Relative changing values of $\bar{H}_j$ and δ_H on scanning stratums 1~4 in silty clay specimen

Scanning stratum	$\Delta\bar{H}'_j$ (%)		$\Delta\delta'_H$ (%)	
	Hardening	Softening	Hardening	Softening
1	2.0	10.3	35.7	462.8
2	2.5	10.2	89.4	249.7
3	2.5	22.5	63.2	410.3
4	2.1	3.0	38.6	298.0

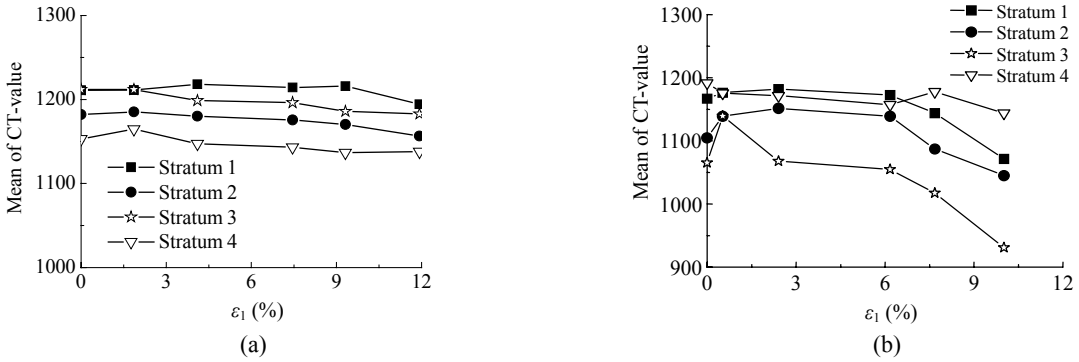

Fig.4 Mean of CT-value of scanning stratums 1~4 ($\bar{H}_j$) in (a) hardening and (b) softening silty clay specimens

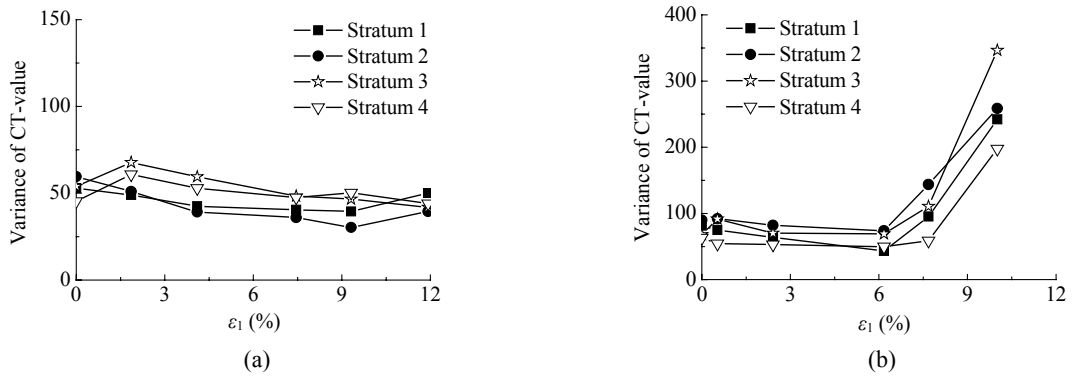

Fig.5 Variance of CT-value of scanning stratums 1~4 (δ_H) in (a) hardening and (b) softening silty clay specimens

Scanning results of special zones

This paper holds this connotation or assumption: a soil specimen keeps a continuum during the compressive loading from the beginning to the end of the test and no strain localization happens. This assumption is consistent with the theoretical basis of DSC (Liu *et al*., 2003). However, we will see that although strain localization happens, the regular statistical variation patterns of CT-value for hardening material manifest corresponding differences compared with those for softening material. The conclusion obtained in the paper remains reasonable.

"Special zones" refer to the naturally mechanical flaw zones inside the specimen, which distribute through the longitudinal section and cross section of the specimen. In Fig.6a, we can see from the CT photogram that all scanning stratums 1~4 have a hi-brightness special zone with a quasi-elliptical shape at the center part of the cross section of the specimen. It is claimed that special zones are composed of micro fissures, cracks, orifices, and grain changes taking place inside the material. Strain localization happens in the special zones. Whatever the reasons for the formation of mechanical flaws at the particle level, these will not be discussed in this paper, but parallelism of the mechanical flaw with a hi-brightness special zone is observed. Fig.6b shows that the areas of special zones in the cross section of the specimen are approximately equal to one another.

From Figs.7~8 we can see that according to the relative changing value of special zones on scanning stratums 1~4, the same regulation appears as follows: the mesoscopic structure of hardening material changes far less than that of softening material. Table 4 gives evidence of the relative changing value of special zones in a hardening silty clay specimen and a softening one. $\Delta\bar{H}'_j$ and $\Delta\delta'_H$ of softening material are three and five times more than those of hardening material, respectively. Relative changing values of hardening material present far less values than those of softening material. The mesoscopic discrepancy of experimental phenomena between hardening material and softening material always exists regardless of whether special zones exist or not.

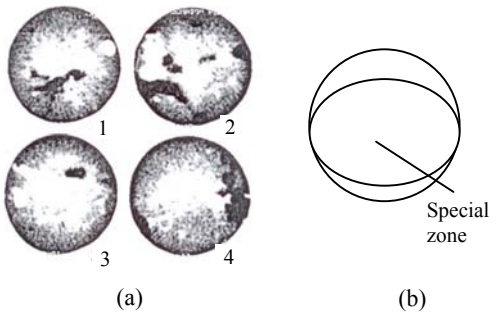

Fig.6 (a) Special zones of scanning stratums 1~4 in the specimen; (b) Sketch of special zones position in the specimen cross section

INTRODUCTION OF MESOSCOPIC STATISTICAL INDEX TO MACROSCOPIC BEHAVIOR PREDICTION

In Eq.(3), the effective plastic deviatoric strain ξ_D is the independent variable of the evolution function of D in general (Desai *et al*., 1991). Sometimes the evolution function of D can be given expression with current shear stress (Desai, 2000) as the independent variable. In this paper CT statistical data is introduced to the evolution function, which materializes the amalgamation of macroscopic and mesoscopic

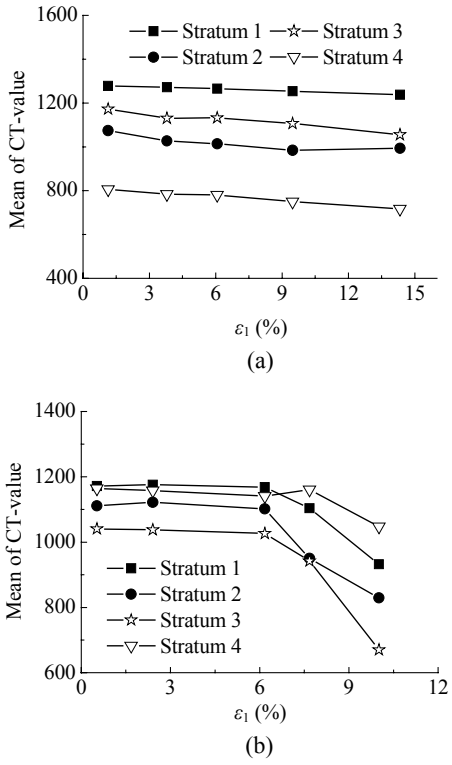

Fig.7 Mean of CT-value of scanning stratums 1~4 ($\bar{H}_j$) on special zones in (a) hardening and (b) softening silty clay specimens

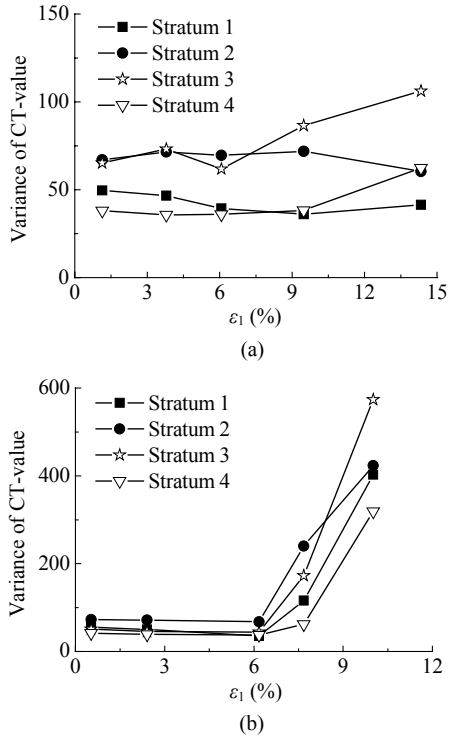

Fig.8 Variance of CT-value of scanning stratums 1~4 (δ_H) on special zones in (a) hardening and (b) softening silty clay specimens

Table 4 Relative changing values of $\bar{H}_j$ and δ_H on scanning stratums 1~4 for special zones in silty clay specimen

Scanning stratum	$\Delta\bar{H}'_j$ (%)		$\Delta\delta'_H$ (%)	
	Hardening	Softening	Hardening	Softening
1	3.4	25.3	38.9	1048.6
2	7.1	35.2	44.1	744.3
3	6.2	55.6	158.5	1023.5
4	5.5	13.6	144.4	625.0

experimental phenomenon measurement methods. The new evolution function makes use of the mesoscopic index to describe macroscopic behavior.

The changing regulation of CT statistical data has a direct connection with hardening or softening behavior of the soils, while the acuity of δ_H changing is associated with the development of D. Accordingly, a new evolution function is constructed as

$$D = D_{\mathrm{u}}(1-\exp(-A(\bar{\delta}_H/10000)^Z)). \tag{12}$$

The specimen has m scanning stratums, and

$$\bar{\delta}_H = \frac{1}{m}\sum_{i=1}^{m}\delta_{Hi}, \tag{13}$$

where $\bar{\delta}_H$ corresponds to the mesoscopic structure changing of the tested material, which takes the same role as ξ_D in Eq.(2). The constant 10000 endows $\bar{\delta}_H$ with the same order of magnitude of ξ_D.

For illustration, by Eq.(1) and Eq.(12), the stress-strain relationship of softening silty clay under 300 kPa lateral compression is computed. RI shares the same hardening response with the same silty clay under 500 kPa lateral compression (Fig.2). Elastics modular of FA equals 0 (Varadarajan *et al*., 2001; Varadarajan and Sharma, 2003). The other required parameters are: A=90, Z=1.18 and D_{u}=0.95. Fig.9 shows that the evolution function containing CT statistical data (i.e., the mesoscopic indices) can be used to provide a fine prediction of material behavior. In Fig.9 a comparison of the DSC result and experimental result shows good agreement. CT scanning was conducted 5~6 times from the very beginning of loading till the material failure occurs. Owning to the limitation of the experimental data extraction frequency, the stress-strain relationship curve in Fig.9 comes out as a broken line.

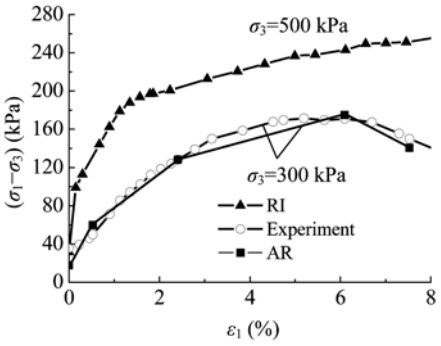

Fig.9 DSC and experimental results comparison of stress-strain relationship of softening silty clay

CONCLUSION

Hardening material shows the characteristics of RI response, i.e., its mesoscopic structure does not change at any stage during applied loading courses, or the changes are negligible. We can assert that

hardening material is material possessing an RI response ability. Softening material has its mesoscopic structure changed prominently. The combination of hardening model utilization and disturbance factor superposition provides the possibility to describe softening response without developing a particular model for softening behavior.

The rationality of softening response depiction by the hardening model is ascertained through the analysis of CT scanning results. The prominent changes of CT statistical data values coincide with the occurrence of disturbance. The mesoscopic phenomenon is coupled with the macroscopic phenomenon: the CT statistical data values for hardening material exhibit mild changes with small quantities and the influence of disturbance can be neglected for hardening behavior depiction. However, the CT statistical data values for softening material change evidently with large quantities and the influence of disturbance must be considered for softening behavior depiction.

The existence of special zones does not affect the mesoscopic phenomenal differences between hardening material and softening material. It is positively acceptable to consider the soil specimen as a continuum while neglecting the existence of special zones.

The introduction of CT statistical data (i.e., the mesoscopic indices) to the evolution function (i.e., the macroscopic relationship expression) puts forward an integrated measurement method from two processes at different levels.

ACKNOWLEDGEMENT

The authors gratefully acknowledge Prof. Xiurun Ge and Prof. Hong Sun for providing the original data.

References

Desai, C.S., 2000. Evaluation of liquefaction using disturbed state and energy approaches. *Journal of Geotechnical and Geoenvironmental Engineering*, **126**(7):618-631. [doi:10.1061/(ASCE)1090-0241(2000)126:7(618)]

Desai, C.S., 2001. Mechanics of Materials and Interfaces—Disturbed State Concept. CRC Press, Boca Raton.

Desai, C.S., Toth, J., 1996. Fully adjusted state constitutive modeling based on stress-strain and nondestructive behavior. *International Journal of Solids and Structures*, **33**(11):1619-1650. [doi:10.1016/0020-7683(95)00115-8]

Desai, C.S., Sharma, K.G., Wathugala, G.W., Rigby, D.B., 1991. Implementation of hierarchical single surface δ_0 and δ_1 model in finite element procedure. *International Journal for Numerical and Analytical Methods in Geomechanics*, **15**(9):649-680. [doi:10.1002/nag.1610150904]

Desai, C.S., Jagannath, S.V., Kundu, T., 1995. Mechanical and ultrasonic anisotropic response of soil. *Journal of Engineering Mechanics ASCE*, **121**(6):744-751. [doi:10.1061/(ASCE)0733-9399(1995)121:6(744)]

Erkens, S., 2002. Asphalt Concrete Response. Delft University Press, Netherlands, p.70-79.

Frantziskonis, G., Desai, C.S., 1987a. Constitutive model with strain softening. *International Journal of Solids and Structures*, **23**(6):733-750. [doi:10.1016/0020-7683(87)90076-X]

Frantziskonis, G., Desai, C.S., 1987b. Analysis of a strain softening constitutive model. *International Journal of Solids and Structures*, **23**(6):751-767. [doi:10.1016/0020-7683(87)90077-1]

Katti, D.R., Desai, C.S., 1995. Modeling and testing of cohesive soil using disturbed state concept. *Journal of Engineering Mechanics ASCE*, **121**(5):648-657. [doi:10.1061/(ASCE)0733-9399(1995)121:5(648)]

Liu, M.D., Cater, J.P., Desai, C.S., 2003. Modeling compression behavior of structured geomaterials. *International Journal of Geomechanics*, **3**(2):191-204. [doi:10.1061/(ASCE)1532-3641(2003)3:2(191)]

Michael, S.K., 2001. A Novel Approach to Predict Current Stress-strain Response of Cement Based Materials in Infrastructure. Ph.D Thesis, the University of Arizona, Tucson, Arizona, p.44-53.

Sun, H., 2002. Damage Development Experimental and Theoretical Meso-scopic-macro-scopic Analysis of Shanghai Clay. Postdoctoral Thesis, Shanghai Jiao Tong University, Shanghai, p.23-35 (in Chinese).

Sun, H., Chen, J.F., Ge, X.R., 2004. Deformation characteristics of silty clay subjected to tri-axial loading by computerized tomography. *Géotechnique*, **54**(5):307-314. [doi:10.1680/geot.54.5.307.46724]

Varadarajan, A., Sharma, K.G., Venkatachalam, K., Gupta, A.K., 2003. Testing and modeling of two rockfill materials. *Journal of Geotechnical and Geoenvironmental Engineering*, **129**(3):206-218. [doi:10.1061/(ASCE)1090-0241(2003)129:3(206)]

Varadarajan, A., Sharma, K.G., Desai, C.S., Hashemi, M., 2001. Constitute modeling of a schistose rock in the Himalaya. *International Journal of Geomechanics*, **1**(1):83-107. [doi:10.1061/(ASCE)1532-3641(2001)1:1(83)]

Wang, D.L., Ge, X.R., 2004. Discussion of some problems about HISS model. *Rock and Soil Mechanics*, **25**(7):1059-1062 (in Chinese).

Wang, G.X., Xiao, S.F., Huang, H.W., Wu, C.Y., 2004. Study of constitutive model of structural clay based on the dis-

turbed state concept. *Acta Mechanica Solida Sinica*, **25**(2):191-197 (in Chinese).

Wu, G., Zhang, L., 2004. Studying unloading failure characteristics of a rock mass using the disturbed state concept. *International Journal of Rock Mechanics and Mining Sciences*, **41**(3):437-443. [doi:10.1016/j.ijrmms.2003.12.077]

Zhang, Y.J., Wang, C.M., Wang, F., Zeng, H.B., 2005. Stress-strain relationship and analysis of compressive deformation of cohesive soil based on DSC. *Global Geology*, **24**(2):200-202 (in Chinese).

Zhou, C., Shen, Z.J., Chen, S.S., Chen, T.L., 2004. A hypoplasticity disturbed state model for structured soils. *Chinese Journal of Geotechnical Engineering*, **26**(4):435-439 (in Chinese).